Mon. Not. R. Astron. Soc. **000**, 000–000 (0000) Printed 21 September 1999 (MN LaTeX style file v1.4)

An improved method of constructing binned luminosity functions

M. J. Page[1], F.J. Carrera[2]
[1] *Mullard Space Science Laboratory, University College London, Holmbury St Mary, Dorking, Surrey RH5 6NT, UK.*
[2] *Instituto de Física de Cantabria (Consejo Superior de Investigaciones Científicas–Universidad de Cantabria), 39005 Santander, Spain.*

ABSTRACT

We show that binned differential luminosity functions constructed using the $1/V_a$ method have a significant systematic error for objects close to their parent sample's flux limit(s). This is particularly noticeable when luminosity functions are produced for a number of different redshift ranges as is common in the study of AGN or galaxy evolution. We present a simple method of constructing a binned luminosity function which overcomes this problem and has a number of other advantages over the traditional $1/V_a$ method. We also describe a practical method for comparing binned and model luminosity functions, by calculating the expectation values of the binned luminosity function from the model.

Binned luminosity functions produced by the two methods are compared for simulated data and for the Large Bright QSO Survey (LBQS). It is shown that the $1/V_a$ method produces a very misleading picture of evolution in the LBQS. The binned luminosity function of the LBQS is then compared to a model two power law luminosity function undergoing pure luminosity evolution from Boyle et al. (1991). The comparison is made using a model luminosity function averaged over each redshift shell, and using the expectation values for the binned luminosity function calculated from the model. The luminosity function averaged in each redshift shell gives a misleading impression that the model over predicts the number of QSOs at low luminosity even when model and data are consistent. The expectation values show that there are significant differences between model and data: the model overpredicts the number of low luminosity sources at both low and high redshift. The luminosity function does not appear to steepen relative to the model as redshift increases.

Key words: Galaxies:luminosity function - galaxies:evolution - galaxies:quasars

1 INTRODUCTION

For three decades considerable effort has been spent in obtaining samples of AGN to investigate their cosmological evolution. This evolution is seen as a change in the luminosity function with redshift. In recent years, galaxy redshift surveys and X–ray cluster surveys have become sufficiently deep that the evolution of galaxies and clusters of galaxies can be examined in the same way as that of AGN. Quantifying and understanding the evolution of these populations is essential to modern cosmology.

A number of methods exist for demonstrating and quantifying the cosmological evolution of a population, eg the $\langle V/V_{max}\rangle$ method of Schmidt (1968) or by comparison with Monte Carlo simulations (La Franca & Cristiani 1997). The simplest, most intuitive method is to construct a binned differential luminosity function in a number of redshift intervals. For flux limited samples (which are the norm in evolution studies), this is usually done using the $1/V_a$ method (eg Maccacaro et al. 1991, Ellis et al. 1996). However, the $1/V_a$ method introduces a significant error for objects close to the flux limit, and hence is *not* the optimum method for constructing binned differential luminosity functions. We present a simple, alternative method which we show is superior to $1/V_a$.

This paper is laid out as follows. Section 2 describes both the $1/V_a$ method, and our new method, for constructing binned differential luminosity functions. The relative merits of the two methods are compared in Section 3, and in Section 4 a Monte Carlo simulation is used to demonstrate the improvement that our method offers over the $1/V_a$ method. In Section 5 we present a technique for comparing binned and model luminosity functions. We apply the two different methods to construct binned luminosity functions of the Large Bright QSO Survey sample in Section 6. In Section 7 this sample is compared to one of the model luminosity functions and evolution laws from Boyle et al. (1991) using both an averaged luminosity function and using the method given in Section 5. Our conclusions are presented in Section 8.

2 METHOD

2.1 Fundamental quantities

We define the differential luminosity function ϕ, of any extragalactic population, as the number of objects per unit comoving volume per unit luminosity interval, i.e.

$$\phi(L,z) = \frac{d^2N}{dVdL}(L,z) \tag{1}$$

where N is the number of objects of luminosity L found in comoving volume V at redshift z. We assume ϕ is a continuous function over the range of redshift and luminosity for which it is defined.

The differential luminosity function is often defined as a function of logarithmic luminosity or (by optical astronomers) magnitude rather than luminosity. The method described here is equally applicable to luminosity functions defined in this way, with the appropriate substitution of 'log (L)' or 'm' where we have used 'L'.

2.2 The $1/V_a$ method

The $1/V_a$ method was originally proposed (Schmidt 1968) to measure space density (dN/dV); the method was generalised for samples with multiple flux limits in Avni & Bahcall (1980). If N objects have luminosities and redshifts in the interval $\Delta L \Delta z$ around the bin centre (L,z):

$$\frac{dN}{dV}(L,z) \approx \sum_{i=1}^{N} \frac{1}{V_a(i)}$$

where $V_a(i)$ is the survey volume in which object i with luminosity $L(i)$ could have been detected and remained in the redshift bin Δz. It is an unbiased estimator of the space density (Felten 1976); the main advantage of this method (compared with simply dividing the number of objects found by the average volume searched) is that it takes account of the fact that more luminous objects are detectable over a larger volume than the less luminous objects.

The $1/V_a$ method is used to estimate ϕ by dividing the space density by the luminosity bin width. We will refer to the approximation of ϕ obtained using this method as ϕ_{1/V_a}:

$$\phi_{1/V_a}(L,z) = \frac{1}{\Delta L}\sum_{i=1}^{N} \frac{1}{V_a(i)} \tag{2}$$

2.3 A binned approximation to ϕ

The luminosity function as defined in equation 1 is related to the expected number of objects found in any region $\Delta L \Delta V(\Delta z)$ of the volume-luminosity plane by

$$\langle N \rangle = \int_{L_{min}}^{L_{max}} \int_{z_{min}}^{z_{max}(L)} \phi(L,z)\frac{dV}{dz} dz dL \tag{3}$$

where z_{min} is the bottom of the redshift interval Δz and $z_{max}(L)$ is the highest redshift possible for an object of luminosity L to be detected and remain in the redshift interval Δz. Angled brackets denote expectation value. If ϕ changes little over $\Delta L \Delta z$, then

$$\langle N \rangle \approx \phi(L,z) \int_{L_{min}}^{L_{max}} \int_{z_{min}}^{z_{max}(L)} \frac{dV}{dz} dz dL \tag{4}$$

It follows that if N objects have been found over some volume-luminosity region A,

$$\phi \approx \phi_{est} = \frac{N}{\int_{L_{min}}^{L_{max}} \int_{z_{min}}^{z_{max}(L)} \frac{dV}{dz} dz dL} \tag{5}$$

where ϕ_{est} is our binned estimate of the luminosity function.

3 COMPARISON OF THE TWO METHODS

3.1 Which is the better estimate of ϕ ?

Consider a single bin, corresponding to the redshift - luminosity interval $\Delta L\ \Delta z$ around the point (L_1, z_1), in a binned luminosity function constructed from a flux limited sample of objects. We assume that ΔL and Δz are sufficiently small and/or that ϕ is a sufficiently slowly varying function of L and z that our single estimate of ϕ is appropriate over the whole interval. Some portion of the region $\Delta L\ \Delta z$ may represent objects which are fainter than the survey flux limit. This situation is illustrated in Fig. 1 where the curve $L = L_{lim}(z)$ represents the flux limit of the survey.

The shaded region in Fig. 1a is that region of the volume luminosity plane in the interval $\Delta L\ \Delta z$ which has been surveyed. This shaded area corresponds to the double integral in equation 4. By definition (equation 5), ϕ_{est} gives a good estimate to $\phi(L_1, z_1)$.

The shaded region in Fig. 1b has an area equal to $(\Delta L\ V_a(i))$ for object i, represented by the black spot. This area is clearly *not* the same as that of the surveyed region (the shaded region in Fig. 1a) and hence there is no guarantee that ϕ_{1/V_a} will give a good estimate of ϕ. However, there are two specific cases in which ϕ_{1/V_a} will always give a good estimate of ϕ:

1) The entire redshift, luminosity interval $\Delta L\ \Delta z$ corresponds to objects brighter than the flux limit of the survey, i.e. in Fig. 1 the curve $L = L_{lim}(z)$ passes above the $\Delta L\ \Delta z$ region. In this case,

$$\int\int dVdL = \Delta L\ \Delta V(\Delta z)$$

and

$$\phi_{1/V_a} = \phi_{est} \approx \phi$$

2) ΔL is very small:

$$\phi_{1/V_a} \approx \frac{1}{\Delta L}\frac{dN}{dV} \rightarrow \frac{d^2N}{dVdL} \quad \text{as} \quad \Delta L \rightarrow 0$$

Note that even in these limiting cases, ϕ_{1/V_a} does not give a better estimate to ϕ than ϕ_{est}; instead ϕ_{1/V_a} and ϕ_{est} have the same value in case 1 and converge to the same value in case 2. Case 1 generally applies for luminosity functions of objects which are much brighter than the flux limits. Hence for luminosity functions in a number

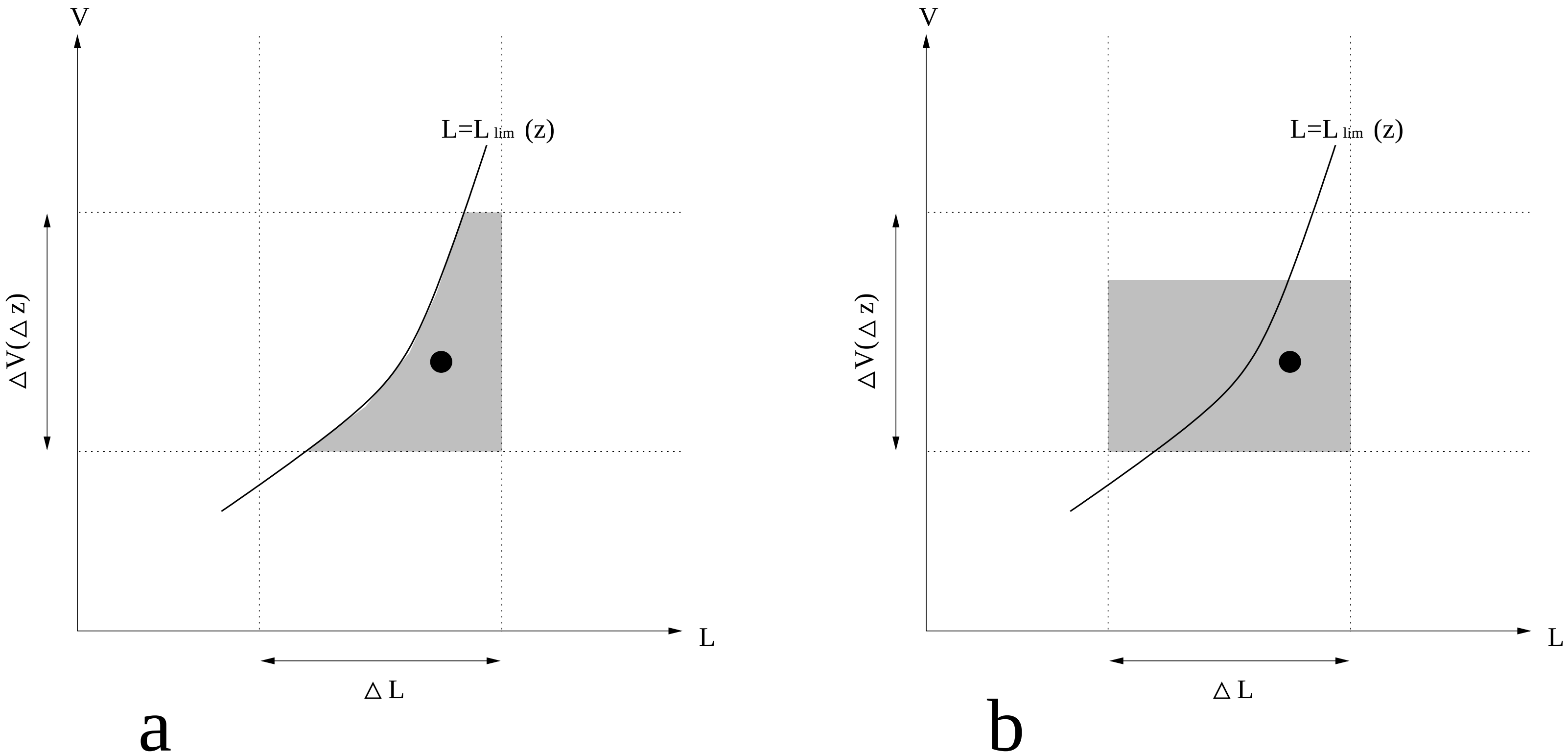

Figure 1. Volume-luminosity space 'available' to an object (the black dot) in (a) ϕ_{est} and (b) ϕ_{1/V_a}. The line L=L$_{lim}(z)$ is the minimum detectable luminosity of an object of redshift z and is determined by the flux limit of the survey.

of redshift intervals, the two methods will produce the same results for the highest luminosity bins of any given redshift shell. At the lowest luminosities in each redshift shell, where objects are close to the survey flux limit and the shaded region of volume-luminosity space in Fig.1a is much smaller than the rectangular $\Delta L \Delta V$ region, the two methods are likely to give the most different results. In all cases, ϕ_{est} can be expected to give as good or better estimates for ϕ than ϕ_{1/V_a}, and is therefore the better estimator.

3.2 Statistical uncertainty in the two methods

From the definition of ϕ_{est} in Section 2.3 it is easily shown that the statistical uncertainty, $\delta\phi_{est}$, is given by:

$$\delta\phi_{est} = \frac{\delta N}{\int_{L_{min}}^{L_{max}} \int_{z_{min}}^{z_{max}(L)} \frac{dV}{dz} dz dL} \qquad (6)$$

where δN is the uncertainty on N objects and can be calculated from Poisson or Gaussian statistics as appropriate.

The statistical uncertainty on ϕ_{1/V_a} is harder to estimate, because each object makes a different statistical contribution. The uncertainty is typically estimated by the following expression:

$$\delta\phi_{1/V_a} = \frac{1}{\Delta L} \sqrt{\sum_{i=1}^{N} \left(\frac{1}{V_a(i)} \right)^2} \qquad (7)$$

(eg Marshall 1985, Boyle et al. 1988) but this assumes Gaussian statistics and therefore is not appropriate for bins containing few objects.

Hence the uncertainty on ϕ_{est} is easily calculated for any number of objects within a bin, but the uncertainty on ϕ_{1/V_a} can only be properly estimated when there are many sources per bin.

3.3 Multiple flux limits

The comparison so far and Fig. 1 has assumed the simple case of a survey with a single flux limit. However, many surveys have different flux limits for different parts of the survey area, and most luminosity function investigations combine different surveys with different flux limits. Indeed, combining large area shallow surveys and small area deep surveys is currently the only practical way to obtain a luminosity function which spans a wide range of luminosities at a wide range of redshifts. The most efficient means to combine areas with different flux limits is to assume that each object could be found in any of the survey areas for which it is brighter than the corresponding flux limit. This is 'coherent' addition of samples in the language of Avni & Bahcall (1980). In this case, it is no longer true that only the lowest luminosity objects in each redshift shell are close to the flux limit, because objects of higher luminosity are close to the flux limit of the shallower survey areas. The problem with ϕ_{1/V_a} therefore affects luminosity bins that correspond to any of the survey flux limits, although the severity of the problem is watered down by the deeper survey areas.

Many surveys also have a *maximum* flux limit beyond which sources are too bright to have been selected. In this case z_{min} in equations 1 - 6, as well as z_{max}, is a function of L. As an illustration, if the curve $L = L_{lim}(z)$ in Fig. 1 were to represent a maximum (rather than a minimum) flux limit, objects would have to lie on the other side of the curve to be included in the survey. If the object (black dot) in Fig. 1 were shifted straight upwards to lie above the black line, it is now the shaded area of Fig. 1a subtracted from $\Delta L\ \Delta V(\Delta z)$ which corresponds to the double integral in equation 4, and the shaded area of Fig. 1b subtracted from $\Delta L\ \Delta V(\Delta z)$. which corresponds to $(\Delta L\ V_a(i))$. Just as for the minimum flux limit (section 3.1), these two quantities are different, and there is no guarantee that ϕ_{1/V_a} will give a good estimate of ϕ. Therefore, for surveys with both bright and faint flux limits, ϕ_{1/V_a} is likely to be inferior to ϕ_{est} at the highest as well as the lowest luminosity bins in each redshift shell.

4 A SIMULATED LUMINOSITY FUNCTION

In this section we use a sample simulated by a Monte Carlo method to demonstrate the improvement that ϕ_{est} offers over the traditional ϕ_{1/V_a}. The simulation was performed using a two power law model X–ray luminosity function which is unchanging with redshift (i.e. no evolution) and a single flux limit. The Monte Carlo simulation produced a source list of ~ 10000 sources. Binned luminosity functions were produced for this simulated data in a range of redshift intervals using both methods. These are shown in Fig. 2, ϕ_{est} on the left and ϕ_{1/V_a} on the right. The model luminosity function is shown as a dashed line.

The two methods are in exact agreement for the high luminosity points of each redshift interval, as expected from Sec 3.1. However, for the lowest luminosity bins of the $0.2 < z < 0.5$ and $0.5 < z < 1.0$ redshift intervals ϕ_{1/V_a} is significantly smaller than the input model, while ϕ_{est} is a good representation of the input model. For the lowest luminosity bin of the $2.0 < z < 2.5$ redshift shell ϕ_{1/V_a} is larger than the input model. We therefore see that for objects close to the flux limit ϕ_{1/V_a} can be too small or it can be too large; in simulations we have performed using different flux limits and luminosity functions ϕ_{1/V_a} is more frequently too small than too large.

5 COMPARING BINNED AND MODEL LUMINOSITY FUNCTIONS

The luminosity function is frequently modelled as some analytical function (eg a broken power law or a Schechter function). Models are sometimes fitted to the binned luminosity function and tested for goodness of fit using χ^2. More often the fit is made to the unbinned data by maximum likelihood (Crawford, Jauncey & Murdoch 1970) and models are tested for overall goodness of fit using a one or two dimensional Kolmogorov Smirnov test (Press et al. 1992). However, even in this latter case, comparison between the binned and model luminosity function is the usual recourse to find out *why* models are rejected, i.e. at which redshifts and luminosities the data and model are inconsistent.

In this comparison, a problem can arise that the model is a continuous function and (for a steep luminosity function) can span a rather large range of values within any one luminosity bin. Similarly, any model luminosity function which is evolving with redshift can have a large range of values for a single luminosity over a redshift interval (although this latter effect can be overcome if the evolution is known or assumed a-priori, eg Mathez et al. 1996, Kassiola & Mathez 1990). The binned luminosity function could be compared to the model luminosity function evaluated at some arbitrary 'middle point' of each luminosity/redshift bin; alternatively some weighted average of the model could be produced for each luminosity redshift bin.

A more valid statistical approach is to compute the expectation value of the binned luminosity function from the model, for each redshift/luminosity bin. In this method, a single, unique, model value is produced for each redshift/luminosity bin, which can be compared to the corresponding binned luminosity function data point. This allows the binned luminosity function to be compared with the model using a statistical goodness of fit test such as χ^2, and/or enables the fitting of a model to the binned luminosity function. This approach is illustrated in this section using the Monte Carlo simulated sample of section 4. First, the formulas for expectation value are given.

5.1 $\langle\phi_{1/V_a}\rangle$

The expectation value of ϕ_{1/V_a} is given by:

$$\langle\phi_{1/V_a}\rangle = \frac{\langle N\rangle}{\Delta L}\int_{L_{min}}^{L_{max}} \frac{1}{V_a(L)}P(L)dL \tag{8}$$

where L_{min} and L_{max} are respectively the minimum and maximum luminosities of objects within the luminosity bin and $P(L)$ is the probability density corresponding to an object of luminosity L. $P(L)$ is given by

$$P(L) = \frac{1}{\langle N\rangle}\int_{z_{min}}^{z_{max}(L)} \phi(L,z)\frac{dV}{dz}dz \tag{9}$$

where z_{min} is the lower limit of the redshift shell and $z_{max}(L)$ is the smaller of the maximum detectable redshift of an object of luminosity L and the top of the redshift shell. $\langle N\rangle$ is given by equation 3. Hence

$$\langle\phi_{1/V_a}\rangle = \frac{1}{\Delta L}\int_{L_{min}}^{L_{max}} \frac{1}{V_a(L)}\int_{z_{min}}^{z_{max}(L)} \phi(L,z)\frac{dV}{dz}dz\, dL \tag{10}$$

5.2 $\langle\phi_{est}\rangle$

From equations 3 and 5, the expectation value of ϕ_{est} is given by:

$$\langle\phi_{est}\rangle = \frac{\int_{L_{min}}^{L_{max}}\int_{z_{min}}^{z_{max}(L)}\phi\frac{dV}{dz}dzdL}{\int_{L_{min}}^{L_{max}}\int_{z_{min}}^{z_{max}(L)}\frac{dV}{dz}dzdL} \tag{11}$$

5.3 $\langle\phi_{1/V_a}\rangle$ and $\langle\phi_{est}\rangle$ for the simulated luminosity function

In Fig. 3 $\langle\phi_{1/V_a}\rangle$ and $\langle\phi_{est}\rangle$ are shown with ϕ_{1/V_a} and ϕ_{est} of the Monte Carlo simulated sample of section 4. Unsurprisingly, the binned luminosity function of the Monte Carlo simulated sample is consistent with the expectation luminosity function derived from the input model. Note that the systematic differences between ϕ_{1/V_a} and ϕ (the

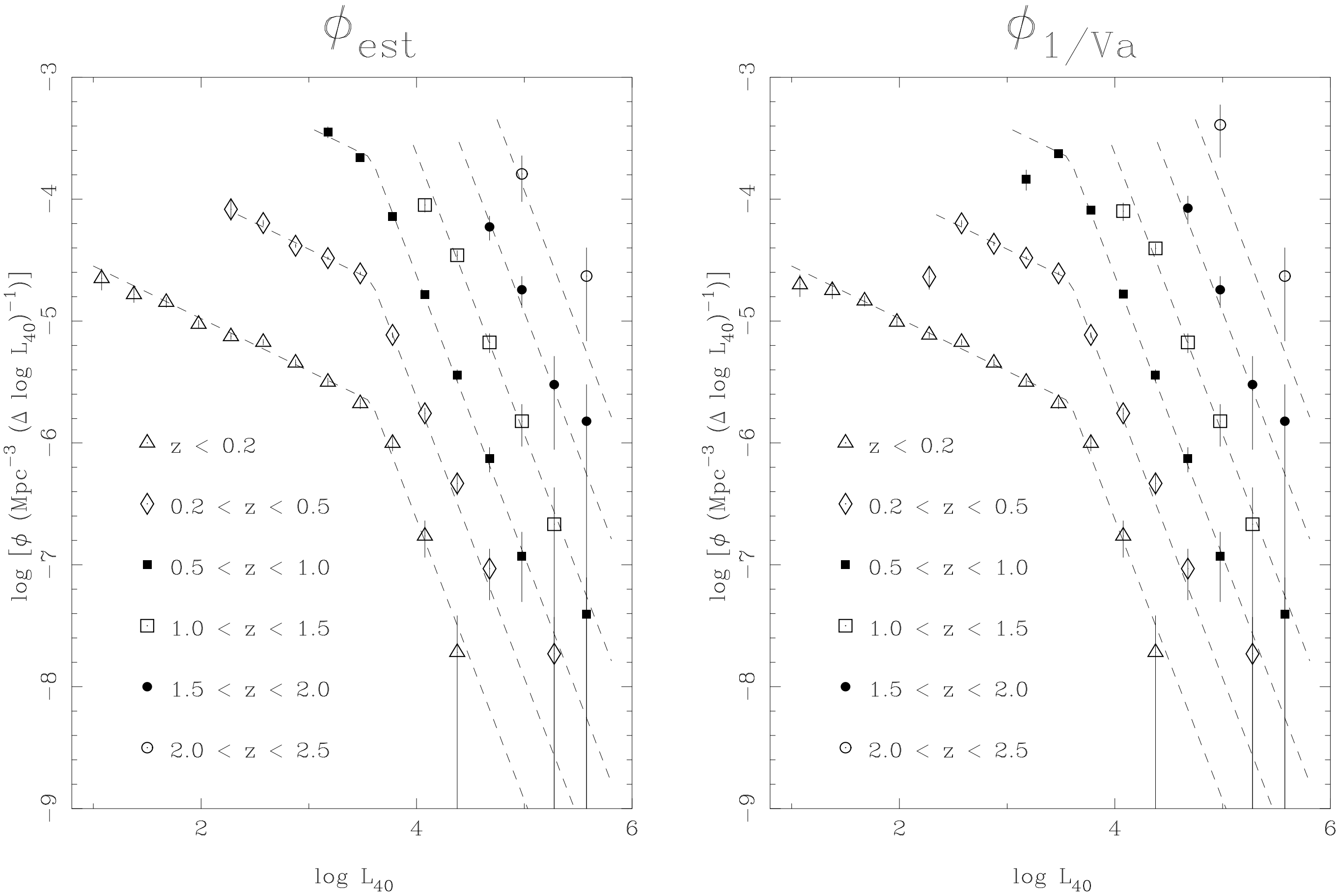

Figure 2. Binned luminosity functions of a simulated sample of objects using (left) ϕ_{est} and (right) ϕ_{1/V_a}. The luminosity functions of successive redshift shells have been shifted in the vertical direction for clarity; the input model has no evolution with redshift and is shown as dashed lines.

turn down of ϕ_{1/V_a} at low luminosities in Fig. 2) are reproduced by $\langle\phi_{1/V_a}\rangle$. Hence it is in principle possible to compare and/or fit a model ϕ to a binned ϕ_{1/V_a} provided that the model is first transformed into $\langle\phi_{1/V_a}\rangle$. However, it is simpler to evaluate equation 11 for arbitrary $\phi(L, z)$ than equation 10, so we are again led to the conclusion that ϕ_{est} is superior to ϕ_{1/V_a}.

6 THE LUMINOSITY FUNCTION OF THE LARGE BRIGHT QSO SURVEY

To demonstrate the difference between binned luminosity functions produced using ϕ_{est} and ϕ_{1/V_a}, we now apply these two methods to real data. For this we have chosen the Large Bright QSO Survey (hereafter LBQS, Hewett, Foltz & Chaffee 1995), the current largest single sample of QSOs available. This is ideal because as samples become larger, the systematic problems with ϕ_{1/V_a} become larger than the statistical uncertainty associated with the data. Note that the LBQS has a maximum flux limit as well as minimum flux limits (see section 3.3); these are given by Hewett et al. (1993).

ϕ_{est} and ϕ_{1/V_a} are shown for the LBQS in Fig. 4 for $q_0 = 0.5$ and H$_0$=50 km s^{-1} Mpc^{-1}. K-correction was performed using the composite spectrum of Cristiani & Vio (1990). The contrast is striking: the ϕ_{1/V_a} binned luminosity function gives the misleading impression that evolution is complex and highly luminosity dependent while ϕ_{est} shows a much simpler picture of the evolution; the latter could be described approximately by pure luminosity evolution.

7 COMPARISON OF THE LARGE BRIGHT QSO SURVEY WITH A MODEL LUMINOSITY FUNCTION

We now compare the binned luminosity function ϕ_{est} of the LBQS with a model luminosity function undergoing pure luminosity evolution. The model chosen is the $q_0 = 0.5$ model from Boyle et al. (1991), which is a two power law luminosity function described by:

$$\phi(M_{B_J}) = \phi^*\{10^{0.4[M_{B_J}-M_{break}(z)](\alpha+1)} + 10^{0.4[M_{B_J}-M_{break}(z)](\beta+1)}\}^{-1}$$

where $\phi^* = 6.5 \times 10^{-7}$ mag^{-1} Mpc^{-3}, $\alpha = -3.9$ and $\beta = -1.5$. The model is subject to pure luminosity evolution such that $M_{break}(z)$=-22.5 - 8.625 log (1+z), until $z = 1.9$ after which $M_{break}(z)$ remains constant at $M_{break}(1.9)$. The binned luminosity function is shown in Fig. 5; the different redshift shells have been placed in separate panels for clarity. For comparison the model is shown as both a volume-weighted average over each redshift shell (dashed

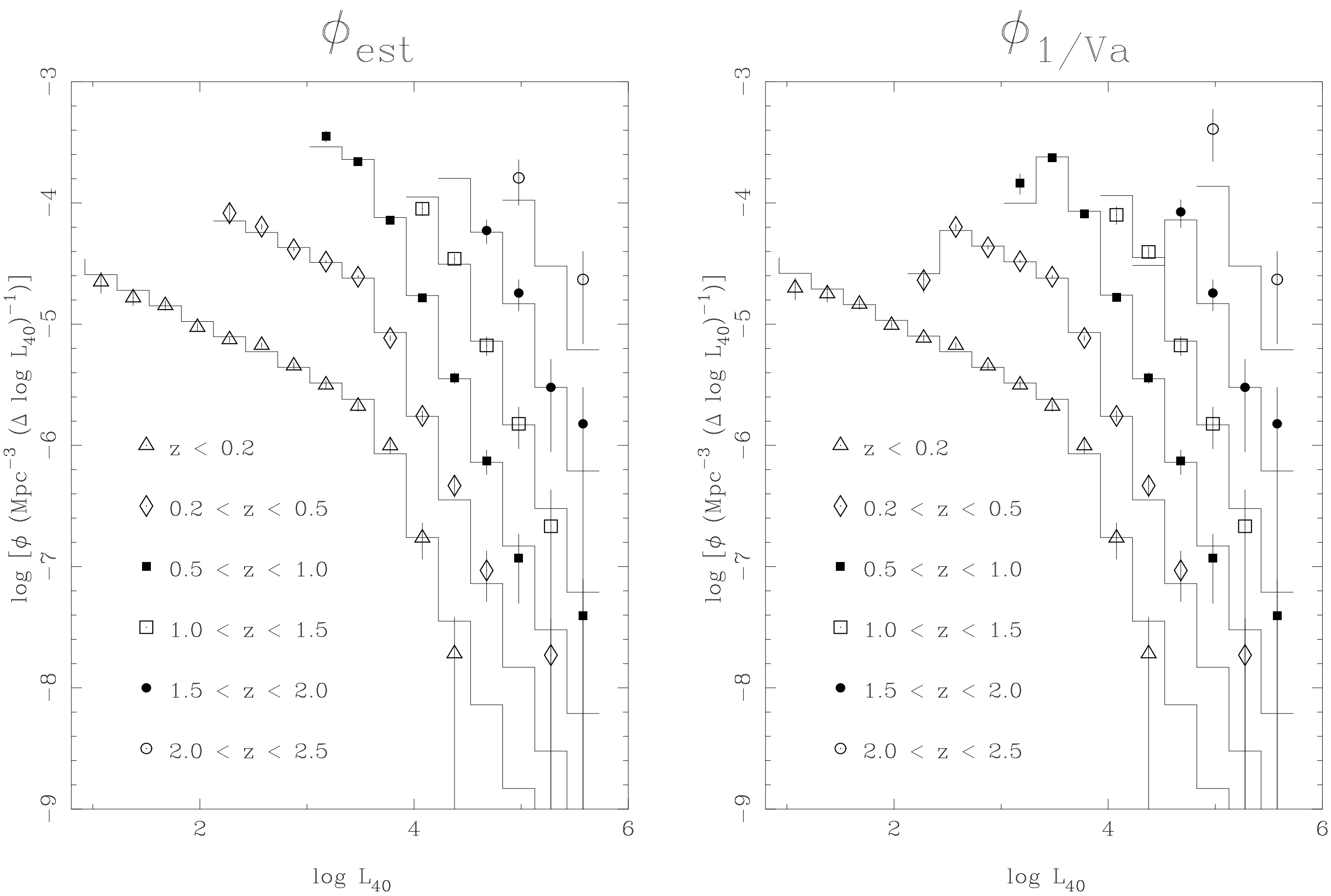

Figure 3. (left): ϕ_{est} (data points) and $\langle\phi_{est}\rangle$ (stepped line) and (right): ϕ_{1/V_a} (data points) $\langle\phi_{1/V_a}\rangle$ (stepped line) for the Monte Carlo simulated sample.

line), and as a set of expectation values $\langle\phi_{est}\rangle$ calculated using Equation 11 (solid stepped line). The two arrows near the bottom of each plot show the position of the 'break' luminosity of the model luminosity function at the top and bottom of the redshift shell.

The advantage of comparing the binned luminosity function to expectation values is well demonstrated by the low luminosity bins of the upper four panels of Fig. 5, in which the continuous volume weighted luminosity function makes the data look far more discrepant than it really is.

The model from Boyle et al. (1991) has already been compared to luminosity function of the LBQS, by Hewett et al. (1993). These authors used cumulative 1/Va luminosity functions in the same redshift shells as used here; these were compared to the model predictions using Kolmogorov Smirnov tests in each redshift shell. Their most important conclusion was that at $z < 2$ the luminosity function systematically steepens relative to the model with increasing z, implying that pure luminosity evolution is no longer a viable model for QSO evolution. Similar claims for other surveys have been made more recently by Goldschmidt & Miller (1998), La Franca & Cristiani (1997) and by Hawkins & Veron (1995).

The binned luminosity function of Fig. 5 does not support this conclusion. Instead, significant discrepancy between data and model at $z < 2$ is always for fainter absolute magnitudes, at or below $M_{break}(z)$, and is always in the sense that the model overpredicts the number of low luminosity sources. To quantify this, we calculated the χ^2 separately for bins brighter, and for bins fainter $M_{break}(z)$ in the four redshift shells at $z < 2$. These are tabulated in Table 1; the lowest and highest luminosity bins of the $0.2 < z < 0.5$ redshift shell and the highest luminosity bin of the $1.0 < z < 1.5$ redshift shell have not been included because they contain too few objects for χ^2 to be appropriate. At absolute magnitudes brighter than $M_{break}(z)$ the model is acceptable at 95%, overall and for each redshift shell individually. At fainter absolute magnitudes the model is significantly deviant for all but the $1.0 < z < 1.5$ redshift shell, and it is notable that in this $1.0 < z < 1.5$ shell the model shows the largest deficiency relative to the data at high luminosities. Although the discrepancy between data and model at low luminosities is sufficient to reject the model at $> 7\sigma$, there is no strong evidence that the luminosity function steepens relative to the model as redshift increases.

8 CONCLUSIONS

We demonstrate that the $1/V_a$ method can lead to systematic errors when used to produce binned differential luminosity functions. This problem is most significant for

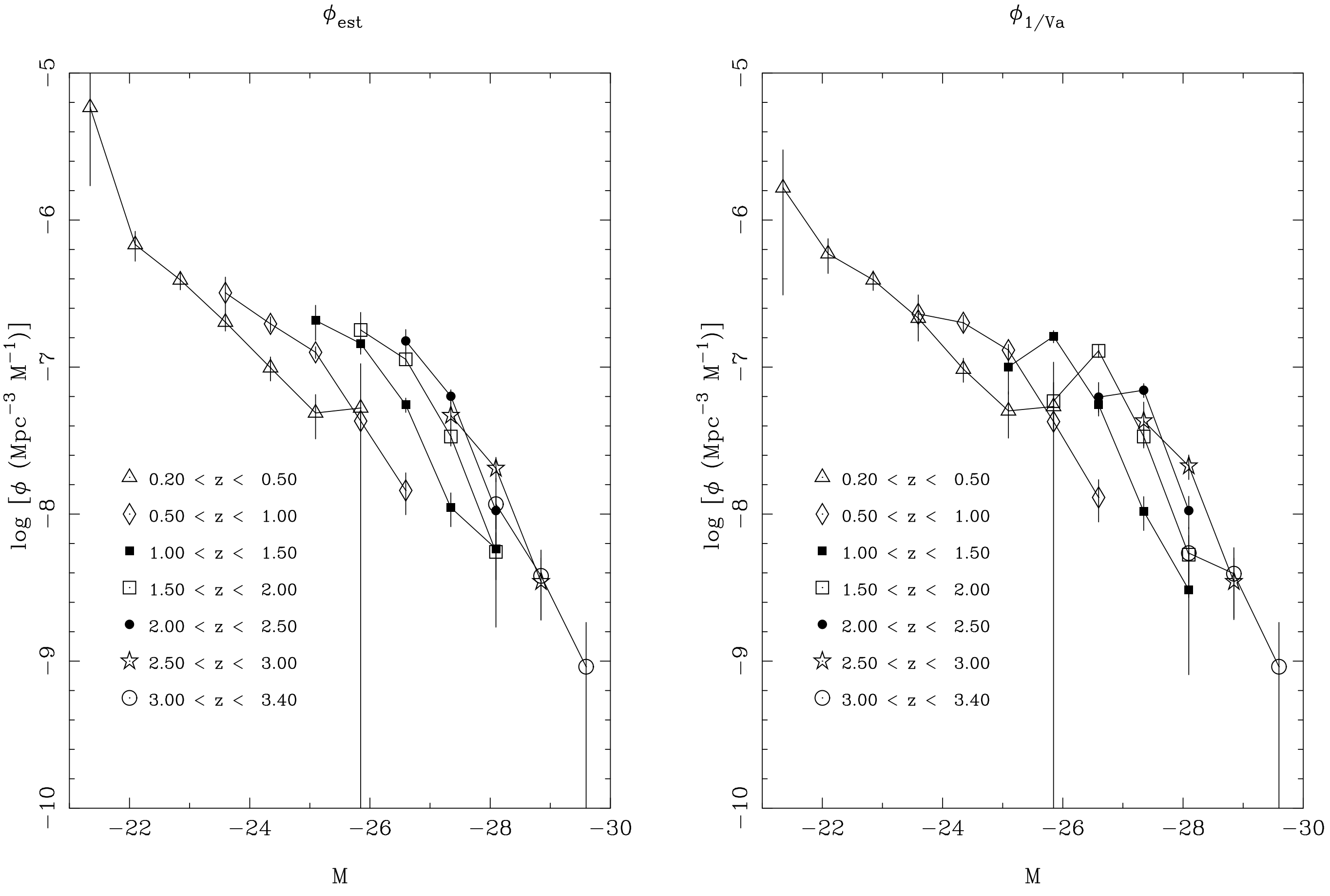

Figure 4. Binned luminosity functions of the LBQS sample: (left) ϕ_{est} and (right) ϕ_{1/V_a}

Table 1. Model goodness of fit at absolute magnitudes brighter, and similar to or fainter than, $M_{break}(z)$ for $z < 2$

	$M_{B_J} < M_{break}(z)$		$M_{B_J} \geq M_{break}(z)$	
Redshift shell	χ^2/ν	P*	χ^2/ν	P*
$0.2 < z < 0.5$	2.89/2	0.24	58.70/3	1.1×10^{-12}
$0.5 < z < 1.0$	3.61/2	0.16	14.72/3	2.1×10^{-3}
$1.0 < z < 1.5$	3.72/2	0.16	0.68/2	0.71
$1.5 < z < 2.0$	3.30/2	0.19	19.21/2	6.7×10^{-5}
Total	13.52/8	0.10	93.31/10	1.2×10^{-15}

* Probability of χ^2 being higher by chance if the data were drawn from the model

objects close to their parent sample's flux limit(s). As a result the lowest luminosity bins of $1/V_a$ luminosity functions which are split by redshift can be unrepresentative, distorting the apparent evolution of extragalactic populations. A new method for constructing binned luminosity functions, which does not have this problem, is presented. The improvement of this new method over the $1/V_a$ method is demonstrated using a Monte Carlo simulated sample of objects. This new method also has the advantages that statistical uncertainty is easily estimated even when there are few objects per bin.

We also present a practical method for comparing binned and model luminosity functions (by eye or by statistical test) which resolves the problem that the model luminosity function has many values within one luminosity-redshift bin.

We demonstrate the difference between the $1/V_a$ method and the new method for constructing binned luminosity functions with the Large Bright QSO Survey sample. Evolution appears complex and highly luminosity dependent when the $1/V_a$ method is used, but relatively simple in the binned luminosity function produced using the new method. We also use the LBQS, along with a model luminosity function and evolution law from Boyle et al. (1991), to demonstrate the advantages of our method for comparing model and binned luminosity functions. We show that the model is inconsistent with the data at low luminosities, but unlike Hewett et al. (1993) we do not find strong evidence that the luminosity function steepens relative to the model as redshift increases.

9 ACKNOWLEDGMENTS

We would like to thank P. Hewitt for supplying the LBQS source list in electronic form and for very useful comments that have improved this paper. FJC thanks the DGES for partial financial support, under project PB95-0122.

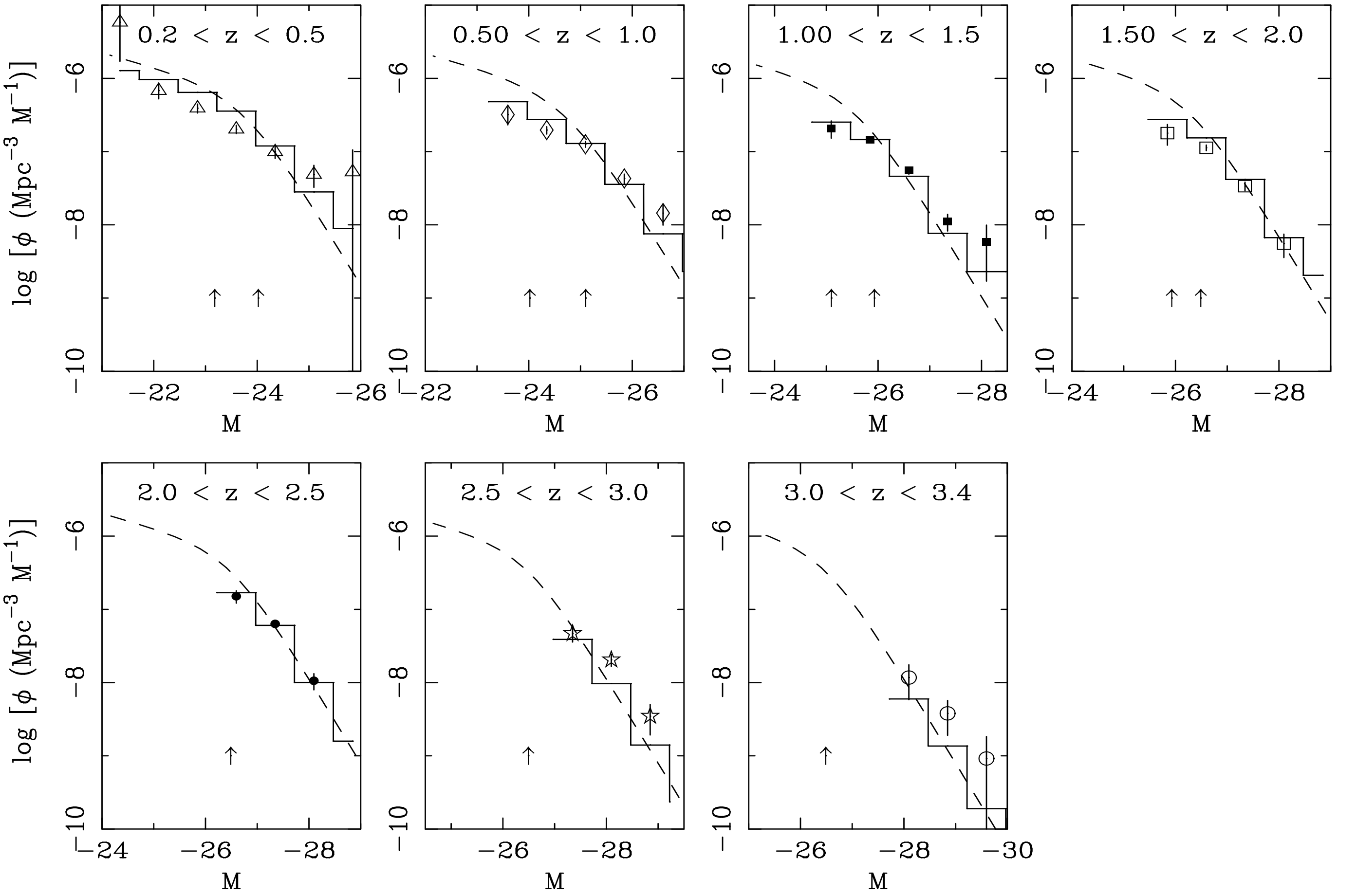

Figure 5. ϕ_{est} for the LBQS (data points) in different redshift shells, with an average model luminosity function (continuous dashed line, see Sec: 7) and $\langle\phi_{est}\rangle$ for the LBQS and the same model (stepped solid line).

10 REFERENCES

Avni Y., and Bahcall J.N., 1980, ApJ, 235, 694

Boyle B.J., Shanks T., Peterson B.A., 1988, MNRAS, 235, 935

Boyle B.J., Jones L.R., Shanks T., Marano B., Zitelli V., Zamorani G., 1991, The Space Distribution of Quasars, ASP Conference Series 21, 191

Cristiani S., & Vio R., 1990, A&A, 227, 385

Crawford D.F., Jauncey D.L. & Murdoch H.S., 1970, ApJ, 162, 405

Ellis R.S., Colless M., Broadhurst T., Heyl J., Glazebrook K., 1996, MNRAS, 280, 235

Felten J.E., 1976, ApJ, 207, 700

La Franca F., Cristiani S., 1997, AJ, 113, 1517

Goldschmidt P., & Miller L., 1998, MNRAS, 293, 107

Hawkins M.R.S., & Veron P., 1995, MNRAS, 275, 1102

Hewett P.C., Foltz C.B., Chaffee F.H., 1993, ApJ, 406, L43

Hewett P.C., Foltz C.B., & Chaffee F.H., 1995, AJ, 109, 1498

Kassiola A. & Mathez G., 1990, A&A, 230, 255

Maccacaro T., Della Ceca R., Gioia I.M., Morris S.L., Stocke J.T., Wolter A., 1991, ApJ, 374, 117

Marshall H.L., 1985, ApJ, 299, 109

Mathez G., Van Waerbeke L., Mellier Y., Bonnet H., Lachièze-Rey M., 1996, A&A, 316, 19

Press W.H., Teukolsky S.A., Vetterling W.T., Flannery B.P., 1992, Numerical Recipes in Fortran, Cambridge University Press

Schmidt M., 1968, ApJ, 151, 393